CCS Chemistry

RESEARCH ARTICLE

Received: Apr. 23, 2019 | Accepted: July 16, 2019

Synthesis of Quaternary Carbon-Centered Benzoindolizidinones via Novel Photoredox-Catalyzed Alkene Aminoarylation: Facile Access to Tylophorine and Analogues

Chao Zhang[1†], Yi Wang[2†], Yugang Song[1†], Hongying Gao[1], Yonghui Sun[1], Xiuyun Sun[1], Yiqing Yang[1], Ming He[1], Zimo Yang[1], Lingpeng Zhan[3], Zhi-Xiang Yu[2*] & Yu Rao[1*]

[1]MOE Key Laboratory of Protein Sciences, School of Pharmaceutical Sciences, MOE Key Laboratory of Bioorganic Phosphorus Chemistry & Chemical Biology, Tsinghua University, Beijing 100084 (China), [2]Beijing National Laboratory for Molecular Sciences (BNLMS), Key Laboratory of Bioorganic Chemistry and Molecular Engineering of Ministry of Education, College of Chemistry, Peking University, Beijing 100871 (China), [3]MOE Beijing National Laboratory for Molecular Sciences, Key Laboratory of Analytical Chemistry for Living Biosystems, Institute of Chemistry, University of Chinese Academy of Sciences, Beijing 100049 (China)

**Corresponding authors: yrao@tsinghua.edu.cn; yuzx@pku.edu.cn; †C.Z., Y.W., and Y.G.S. contributed equally to this work.*

Cite this: *CCS Chem.* **2019**, *1*, 352–364

Photoredox-catalyzed aminoarylation and thioamination of unactivated alkenes have been developed, providing novel synthetic routes to access synthetically challenging quaternary carbon-centered benzoindolizidinones and trifluoromethylthiolated piperidines using readily available starting materials. Notably, these transformations were enabled by merging amidyl radical generation from *N*-alkyl benzamides with oxidant incorporation. Density functional theory calculations were performed to understand the reaction mechanism and to rationalize the regioselectivities. Moreover, the newly developed catalytic aminoarylation provided a convenient synthetic route for natural product tylophorine and its *gem*-dimethyl analogues with greatly improved drug-like properties such as enhanced solubility and stability.

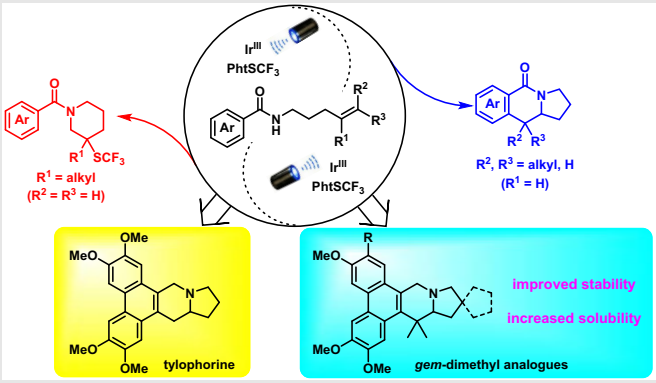

Keywords: photoredox catalysis, alkene aminoarylation, alkene thioamination, amidyl radical, proton-coupled electron transfer, benzoindolizidinone, tylophorine

DOI: 10.31635/ccschem.019.20190018
CCS Chem. **2019**, *1*, 352–364

Introduction

N-Heterocycles serve as important structural motifs in natural products and bioactive molecules.[1,2] Due to their significance in the pharmaceutical industry and biomedical research, development of efficient and practical methods enabling facile access to these heterocycles remains an area of tremendous research efforts.[3,4] Nitrogen radicals,[5–32] amidyl radicals in particular,[13–32] are highly valuable synthetic intermediates for C–N bond-forming reactions, which have been used widely in N-heterocycle synthesis. However, traditional approaches for generating amidyl radicals were usually restricted to the scission of prefunctionalized N–X (X = Cl, Br, O, N, etc.) bonds and harsh reaction conditions.[5] Additionally, the prefunctionalized groups were often incorporated into the target products and were not amenable to the direct construction of C–C bonds, which severely limited the practicability of amidyl radical chemistry. Recently, silver-catalyzed oxidative generation of amidyl radicals from various secondary amides has been applied successfully into aminofluorination of unactivated alkenes.[25] Moreover, some electrochemical methods have also been developed and provided accessible routes for the generation of amidyl radicals from N–H precursors, employed for promoting aminoarylation of alkenes and alkynes.[26–32]

Besides these methods, chemical transformations, based on visible light photoredox catalysis, have received considerable attention in recent years, because of their provision of environmentally benign way to access free-radical intermediates under mild reaction conditions.[33–38] Visible-light-mediated homolytic cleavage of amidyl N–H bond via proton-coupled electron transfer (PCET)[39,40] has provided a straightforward approach for amidyl radical formation with readily available amide substrates. In 2015, Knowles group reported the catalytic alkene carboamination[13] and hydroamidation[14] through homolyzing the N–H bonds of *N*-aryl amides (N–H bond dissociation free energies [BDFEs]: ca. 100 kcal/mol) (Scheme 1a). In 2016, Knowles[15] and Rovis[16,17] groups independently achieved photoredox-catalyzed amidyl radical generation by activating the challenging N–H bonds of *N*-alkyl amides (N–H BDFEs: ca. 110 kcal/mol), which was unrealizable by applying the conventional hydrogen atom transfer approaches (Scheme 1b). More recently, Knowles group developed a catalytic alkene hydroamination reaction enabled by the PCET activation of *N*-alkyl sulfonamides (N–H BDFEs: ca. 97–105 kcal/mol) (Scheme 1c).[18] All of these reactions proceeded through a concerted PCET or a stepwise deprotonation/oxidation process with the aid of a base under redox-neutral conditions.

Benzoindolizidine scaffolds are present in many polycyclic alkaloids (Figure 1).[41] These characteristic skeletons have attracted widespread attention because of their potent and diverse biological activities. A typical example is tylophorine, which exhibits various biological activities including antitumor, antispasmodic, anti-inflammatory, and antimicrobial effects.[42–44] So far, synthetic routes for

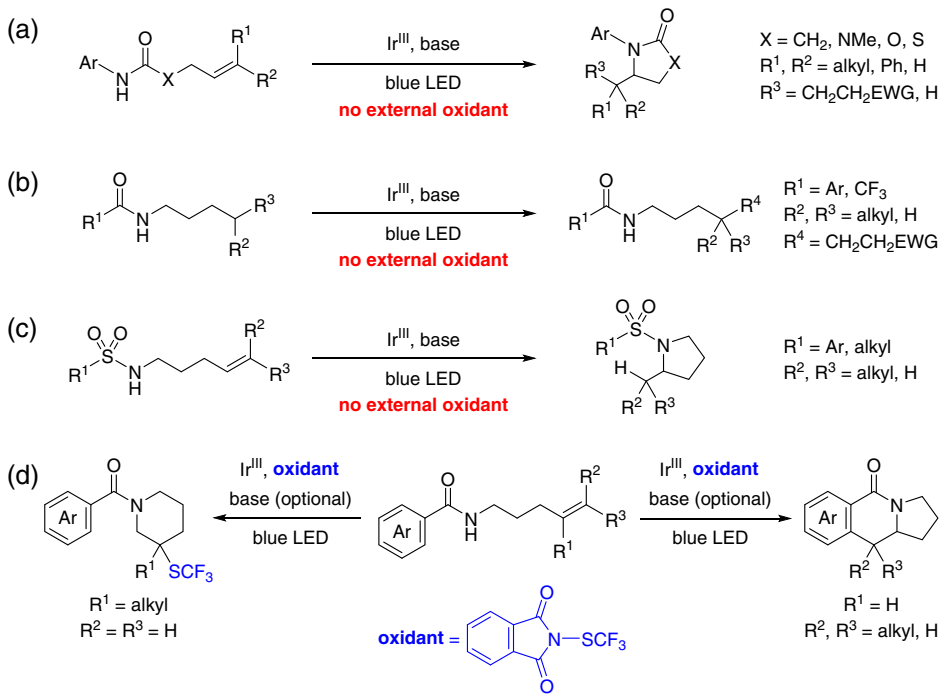

Scheme 1 | *Visible-light-mediated generation and application of amidyl radicals. (a–c) Previous reports by Knowles and Rovis groups, compared with (d) this work.*

DOI: 10.31635/ccschem.019.20190018
CCS Chem. **2019**, *1*, 352–364

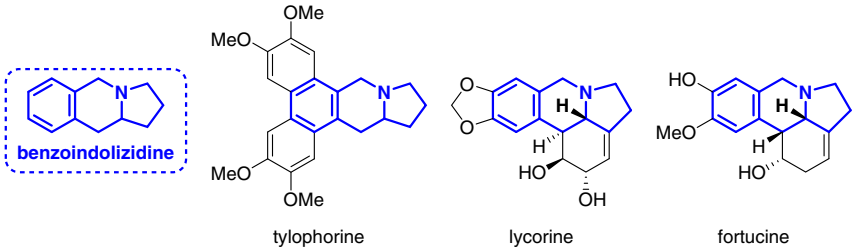

Figure 1 | *Benzoindolizidine alkaloids.*

benzoindolizidine scaffolds, such as transition-metal-catalyzed carbonylation of amines and alkene aminoarylations, were frequently confined to multiple steps, elevated temperatures, or difficulties encountered in accessing the starting materials.[45–47] Besides, metals used in these reactions were subject to protodemetallation or β-hydride elimination, which could hinder the formation of the desired C–C bond.[48] Moreover, the scope of the reported aminoarylations was restricted to monosubstituted alkenes.[45,47] Therefore, developing a general and efficient synthetic method for benzoindolizidines is still in high demand.

To solve this problem, we sought to generate amidyl radicals from *N*-alkyl benzamides using photoredox catalysis and apply these reactive radical intermediates into benzoindolizidine synthesis.[45] As postulated in Figure 2a, following a photo-mediated PCET activation of the N–H bond of benzamide **I** with an excited-state Ir^{III} species, amidyl radical **II** and an Ir^{II} intermediate would be generated. However, due to the facile back electron transfer (BET) between **II** and the reduced form of the photocatalyst, the quantum efficiency of photoredox catalysis is low.[49] We presumed that the introduction of an external oxidant might convert the Ir^{II} species into its Ir^{III} state (Figure 2b). As a result, the BET between **II** and Ir^{II} would be largely prevented. In such a case, the productive 5-*exo*-trig cyclization of **II** would take place to generate alkyl radical **IV**, which might participate in the subsequent intramolecular radical addition to afford delocalized radical intermediate **V** (Figure 2c). Subsequently, **V** could be aromatized into benzoindolizidinone **VI**. Finally, **VI** could be further converted into benzoindolizidine **VII** through a simple reduction reaction.

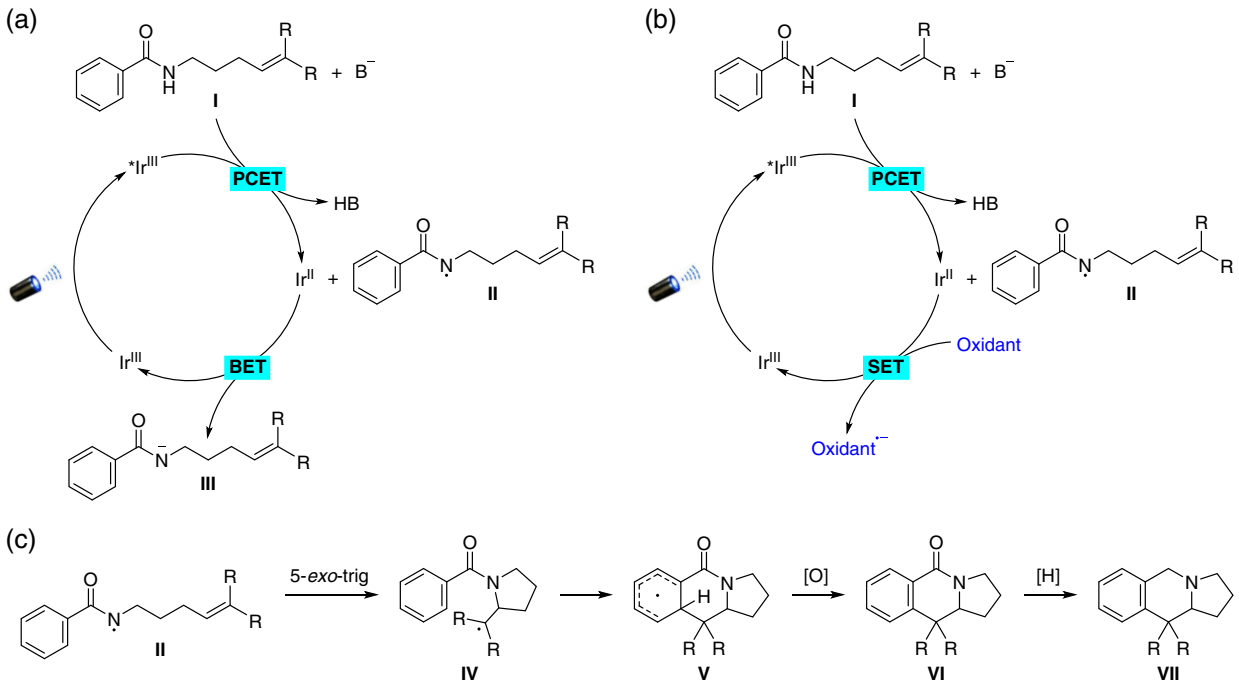

Figure 2 | *Reaction design. (a) Back electron transfer (BET) pathway under redox-neutral conditions. (b) Amidyl radical generation in the presence of an external oxidant. (c) Radical cascade cyclization for benzoindolizidine synthesis. PCET, proton-coupled electron transfer; SET, single-electron transfer.*

DOI: 10.31635/ccschem.019.20190018
CCS Chem. **2019**, *1*, 352–364

Herein, we report the first photoredox-catalyzed alkene aminoarylation and thioamination using *N*-alkyl benzamides (Scheme 1d). The substitution pattern of the substrates could nicely tune regioselectivity through 5-*exo*- and 6-*endo*-trig cyclizations, providing facile routes for the construction of functionalized benzoindolizidinone and piperidine skeletons, respectively. Density functional theory (DFT) calculations were performed to understand the reaction mechanism and to rationalize the regioselectivities. Moreover, the newly developed photoredox-catalyzed alkene aminoarylation was successfully applied to the total synthesis of natural product tylophorine and its *gem*-dimethyl analogues.

Results and Discussion

Reaction Development

As illustrated in Table 1, 4-methoxy-*N*-(5-methylhex-4-en-1-yl)benzamide (**1a**) was exploited as the model substrate with 2 mol % of photocatalyst [Ir(dF(CF_3)ppy)$_2$(dCF_3bpy)]PF_6 (**A**; dF(CF_3)ppy = 3,5-difluoro-2-(5-(trifluoromethyl)pyridin-2-yl)phenyl; dCF_3bpy = 5,5′-bis(trifluoromethyl)-2,2′-bipyridine) and 5 mol % of tetrabutylammonium dibutyl phosphate. Oxygen was chosen as the oxidant in the beginning. Though most of the starting materials were decomposed, to our

Table 1 | *Optimization Studies*

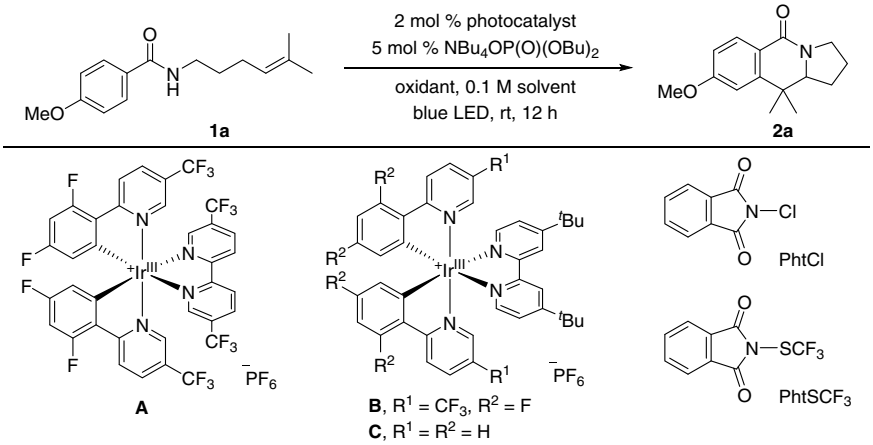

Entry	Photocatalyst	Oxidant (equiv)	Solvent	Yield (%)[a]
1	**A**	O_2 (1 atm)	$PhCF_3$	3
2	**A**	PhtCl (1.0)	$PhCF_3$	11
3	**A**	$K_2S_2O_8$ (1.0)	$PhCF_3$	30
4	**A**	NFSI (1.0)	$PhCF_3$	28
5	**A**	$PhtSCF_3$ (1.0)	$PhCF_3$	50
6	**A**	$PhtSCF_3$ (1.5)	$PhCF_3$	68
7[b]	**A**	$PhtSCF_3$ (2.0)	$PhCF_3$	80 (76)[c]
8	**A**	$PhtSCF_3$ (2.0)	CH_2Cl_2	42
9	**A**	$PhtSCF_3$ (2.0)	THF	45
10	**A**	$PhtSCF_3$ (2.0)	CH_3CN	ND
11	**B**	$PhtSCF_3$ (2.0)	$PhCF_3$	2
12	**C**	$PhtSCF_3$ (2.0)	$PhCF_3$	9
13	/	$PhtSCF_3$ (2.0)	$PhCF_3$	ND
14[d]	**A**	$PhtSCF_3$ (2.0)	$PhCF_3$	ND
15[b,e]	**A**	$PhtSCF_3$ (2.0)	$PhCF_3$	50 (49)[c]
16[e,f]	**A**	$PhtSCF_3$ (2.0)	$PhCF_3$	59 (57)[c]

[a]Yield determined by ^{1}H NMR analysis using 4-nitrobenzaldehyde as the internal standard. 0.05 mmol scale.
[b]0.1 mmol scale.
[c]Isolated yield.
[d]Without light.
[e]Without $NBu_4OP(O)(OBu)_2$.
[f]0.2 mmol scale, 36 h.
LED = light-emitting diode. **A** = [Ir(dF(CF_3)ppy)$_2$(dCF_3bpy)]PF_6. **B** = [Ir(dF(CF_3)ppy)$_2$(dtbbpy)]PF_6. **C** = [Ir(ppy)$_2$(dtbbpy)]PF_6. dF(CF_3)ppy = 3,5-difluoro-2-(5-(trifluoromethyl)pyridin-2-yl)phenyl. dCF_3bpy = 5,5'-bis(trifluoromethyl)-2,2'-bipyridine. dtbbpy = 4,4'-bis(*tert*-butyl)-2,2'-bipyridine. ppy = 2-(pyridin-2-yl)phenyl. Pht = *N*-phthalimidyl. NFSI = *N*-fluorobenzenesulfonimide. ND = Not detected.

DOI: 10.31635/ccschem.019.20190018
CCS Chem. **2019**, *1*, 352–364

delight, the desired benzoindolizidinone product **2a** could be obtained, albeit in 3% yield (Table 1, entry 1). When PhtCl (Pht = *N*-phthalimidyl) was used as the oxidant, the desired product was obtained in 11% yield (Table 1, entry 2). Further optimization, performed through switching of the oxidant to $K_2S_2O_8$, improved the reaction yield to 30% (Table 1, entry 3), and the choice of *N*-fluorobenzenesulfonimide gave a comparable yield (Table 1, entry 4). Notably, further improvement was observed in the presence of $PhtSCF_3$, furnishing **2a** in 50% yield (Table 1, entry 5). It should be noted that the amount of $PhtSCF_3$ played a critical role in promoting the cyclization process. We were pleased to find that the yield could be increased to 68% when 1.5 equiv $PhtSCF_3$ were added (Table 1, entry 6). Further, increasing the amount of $PhtSCF_3$ to 2.0 equiv enhanced the reaction efficiency with 80% yield (Table 1, entry 7; 76% isolated yield). Other solvents (CH_2Cl_2, THF, and CH_3CN) or Ir catalysts (**B** and **C**) all gave inferior results (Table 1, entries 8–12). Moreover, no desired product was observed in the absence of Ir catalysts or light (Table 1, entries 13 and 14). Interestingly, we still got **2a** in 50% yield (49% isolated yield) without the addition of $NBu_4OP(O)(OBu)_2$ (Table 1, entry 15), and the yield could be increased to 59% (57% isolated yield) with a prolonged reaction time (Table 1, entry 16).

With these determined optimal reaction conditions in hand (Table 1, entry 7), we first examined the scope of *N*-alkyl amides with different benzoyl groups. As illustrated in Figure 3a, a wide range of quaternary carbon-centered benzoindolizidinones (**2a**–**2o**) was constructed

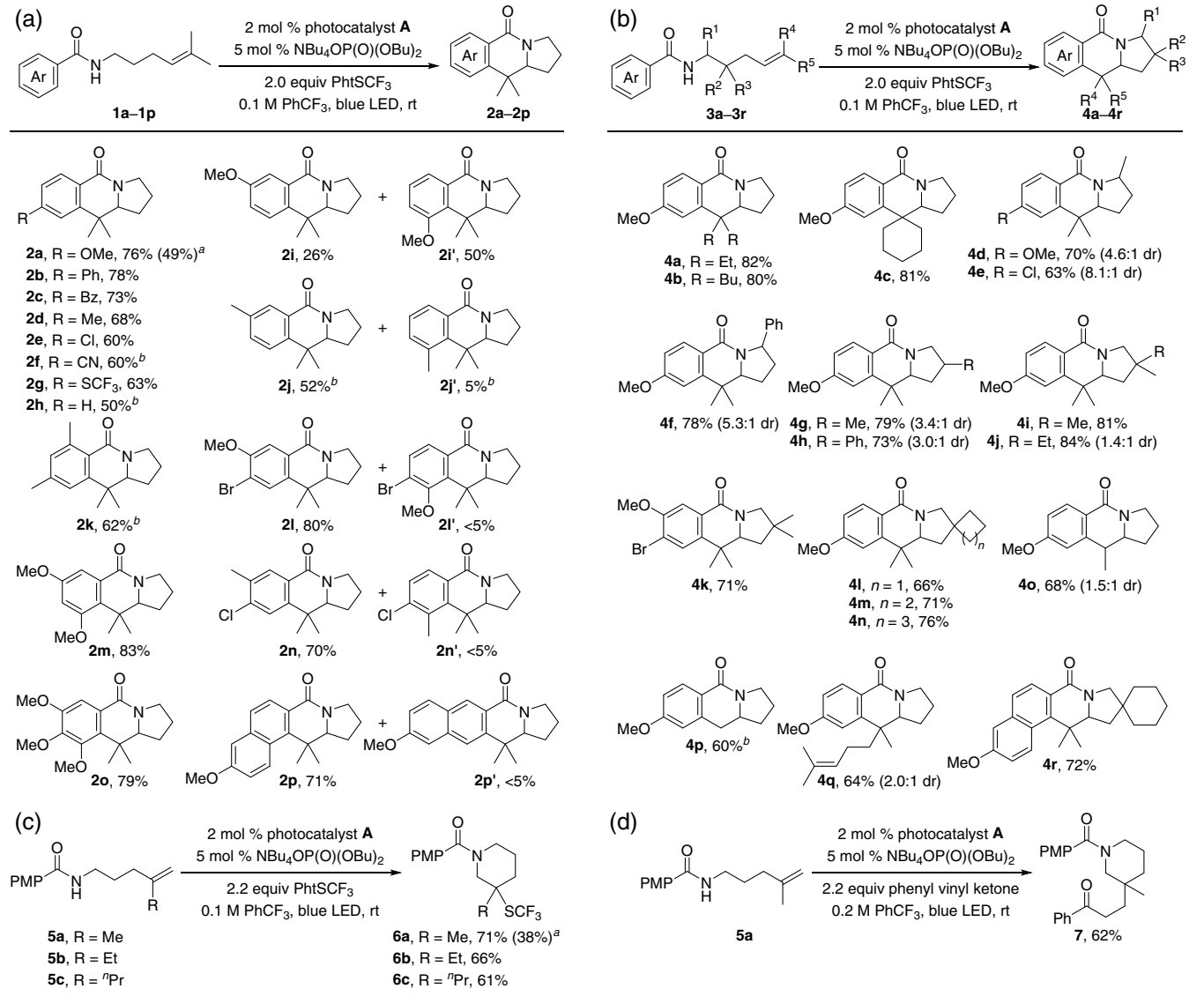

Figure 3 | *Reaction scope. Isolated yields. 0.1 mmol scale. (a, b) Catalytic alkene aminoarylation. (c) Catalytic alkene thioamination. (d) Catalytic alkene carboamination with phenyl vinyl ketone. [a]Without $NBu_4OP(O)(OBu)_2$. [b]0.2 mmol scale. dr, diastereomeric ratio.*

DOI: 10.31635/ccschem.019.20190018
CCS Chem. **2019**, *1*, 352–364

effectively in moderate to good yields. Benzamides containing both electron-rich (OMe, Ph, and Me) and electron-deficient (benzoyl, Cl, CN, and SCF_3) substituents on the phenyl rings were well tolerated (**2a**–**2g**). Besides the *para*-substituted benzoyl groups, nonsubstituted benzoyl group also served as an acceptable group, affording the desired cyclization product **2h** in 50% yield. *N*-alkyl amides with *meta*-methoxybenzoyl and *meta*-methylbenzoyl groups were suitable substrates as well, providing products with different regioselectivities (**2i′** and **2j**). Furthermore, di- and trisubstituted benzoyl groups were also compatible with the reaction conditions, affording a series of polysubstituted benzoindolizidinones **2k**–**2o**. Notably, when substrate **1k** with a sterically hindered *ortho*-methyl group was employed, the desired product **2k** could also be obtained in 62% yield. Finally, 6-methoxy-2-naphthoyl substrate **1p** effectively provided tetracyclic product **2p** in 71% yield under the standard conditions.

Then we investigated the scope with respect to the amino group (Figure 3b). Both diethyl and dibutyl substituted olefins could be used to effectively furnish the cyclized quaternary carbon-centered products in excellent yields (**4a** and **4b**). Notably, the spirocyclic product **4c**, which was difficult to synthesize using traditional methods, was obtained in 81% yield under the standard conditions. Substrates with a substituent at the α-position to the nitrogen atom were used successfully for this reaction, furnishing the corresponding products **4d**–**4f** in moderate to good yields. Similarly, *N*-alkyl benzamides with one or two substituents at the β-position to the nitrogen atom were also competent in the reaction, providing products **4g**–**4k** in good yields. We found that this method was also applicable for the synthesis of spiro compounds **4l**–**4n** with two quaternary carbon centers. Other than trisubstituted olefins, the reaction conditions were feasible for 1,2-disubstituted and monosubstituted olefins as well as a substrate containing two electronically similar alkenes, which afforded various types of benzoindolizidinone compounds (**4o**–**4q**). Notably, a complex pentacyclic spiro compound **4r** with two quaternary carbon centers could be obtained under photoredox catalysis, demonstrating the potential advantages of our current method over the conventional approaches.

As depicted in Figure 3c, to our delight, we found that 1,1-disubstituted olefins **5a**–**5c** demonstrated a different 6-*endo*-trig cyclization mode, affording trifluoromethylthiolated piperidines **6a**–**6c**. It is worth mentioning that we could also obtain product **6a** in the absence of $NBu_4OP(O)(OBu)_2$. Besides alkene thioamination, substrate **5a** proceeded well with phenyl vinyl ketone in a catalytic alkene carboamination, furnishing a quaternary carbon-centered piperidine derivative **7** in 62% yield (Figure 3d).

Mechanistic Studies

We then turned our attention to the reaction mechanism. Substrate **3o** with an *E* configuration provided **4o** as a 1.5:1 mixture of diastereomers under the standard conditions (Scheme 2a). In addition, when an iodo-substituted substrate **1q** was used, the desired product **2q** was formed in 30% yield, and deiodinated product **2j** was also isolated in 10% yield (Scheme 2b). These phenomena indicate that the reaction might have proceeded through a radical mechanism.

Further, we investigated the composition of the byproducts (Scheme 2c). Under the standard conditions, except for product **2a**, bis(trifluoromethyl)disulfide was detected by ^{19}F NMR analysis, and phthalimide (PhtH) was isolated in 94% yield (calculated for 2.0 equiv). Generally, the visible-light-mediated generation of amidyl radicals requires the cooperation of an oxidant, such as an excited-state Ir^{III} complex and a base.[13–18] However, in the absence of the base, $NBu_4OP(O)(OBu)_2$, we found that the reaction still afforded the desired product **2a** in 49% yield, together with bis(trifluoromethyl)disulfide and PhtH (Scheme 2c). These observations indicate that, in the absence of $NBu_4OP(O)(OBu)_2$, the reaction might have proceeded through a different mechanism, compared with the previous works by Knowles and Rovis groups.[13–18]

To further understand the reaction mechanism in the absence of $NBu_4OP(O)(OBu)_2$, we performed some additional control experiments. First, we envisioned that the oxidation of the $^*Ir^{III}$ intermediate ($^*Ir^{III}/Ir^{IV}$ = −0.43 V vs SCE in MeCN[15]) to the Ir^{IV} intermediate by $PhtSCF_3$ (−0.80 V vs SCE in MeCN)[50] was unlikely to be operative according to the redox potentials. Indeed, under the irradiation of blue light, photocatalyst **A** and $PhtSCF_3$ did not react (Scheme 2d), which is in accordance with the Stern–Volmer fluorescence-quenching experiments performed by Glorius group (no reaction between photocatalyst **B** and $PhtSCF_3$ occurred under irradiation).[51,52] Furthermore, neither could the reaction of **1a** and $PhtSCF_3$ take place under irradiation (Scheme 2e). Finally, the luminescence-quenching experiment between photocatalyst **A** and **1a** revealed that the direct electron transfer between the excited state of photocatalyst **A** and **1a** is thermodynamically unfavorable (Scheme 2f). These results demonstrated that the reaction of $^*Ir^{III}$, $PhtSCF_3$, and **1a** should be a three-component process.

Such a three-component reaction might have been initiated by the activation of either alkenyl or amidyl group of **1a**. To understand where the reaction started, we investigated two model substrates **8a** and **8b**, which lacked the amide and alkene moieties of **1a**, respectively. No reaction of alkene **8a** occurred (Scheme 2g), which accorded with the fact that the electron transfer between a trisubstituted alkene (e.g., +1.98 V vs SCE for 2-methylbut-2-ene[53]) and the excited state of photocatalyst **A** ($^*Ir^{III}/Ir^{II}$ = +1.68 V vs SCE in MeCN[15]) was

DOI: 10.31635/ccschem.019.20190018
CCS Chem. **2019**, *1*, 352–364

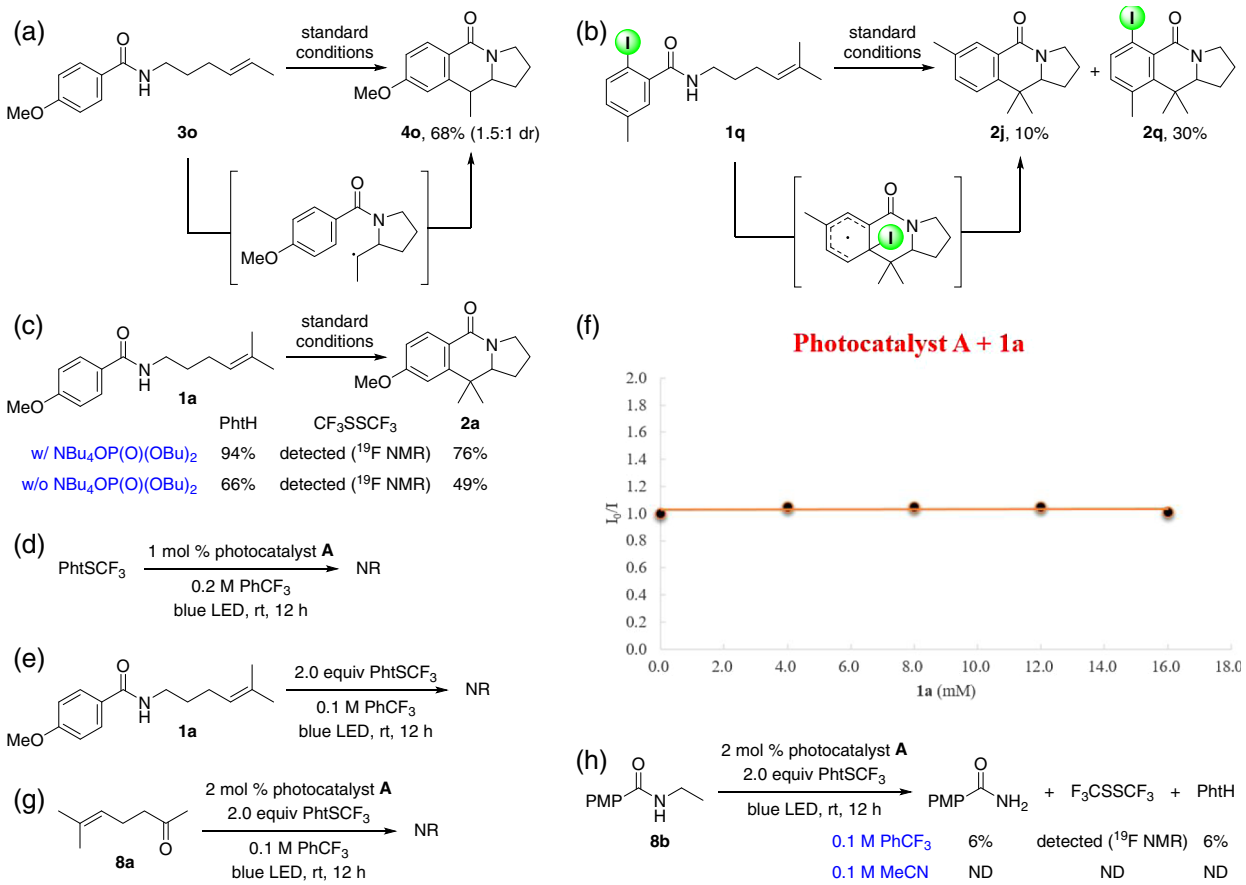

Scheme 2 | *Mechanistic experiments. (a, b) Evidence for a radical mechanism. (c) Investigation of the by-products. (d) The reaction of PhtSCF$_3$ with photocatalyst **A** under irradiation. (e) The reaction of **1a** with PhtSCF$_3$ under irradiation. (f) Stern–Volmer luminescence-quenching study between photocatalyst **A** and **1a**. (g) The reaction of **8a** under irradiation. (h) The reaction of **8b** under irradiation. NR, no reaction; ND, not detected.*

endergonic by ca. 0.3 V. In contrast, we found that amide **8b** was converted into 4-methoxybenzamide under photoredox catalysis (Scheme 2h). PhtH and CF_3SSCF_3 derived from PhtSCF$_3$ were also detected. These results suggested that the reaction initiated plausibly with the activation of the amide moiety.

Based on the above preliminary experimental results, we proposed a possible mechanism for amidyl radical generation in the absence of $NBu_4OP(O)(OBu)_2$ (Figure 4a). Though the oxidation potential of amide **8b** (+1.86 V vs SCE in MeCN[15]) is higher than the excited-state reduction potential of photocatalyst **A** (+1.68 V vs SCE in MeCN[15]), we postulated that an amide substrate such as **1a** and **8b** might be oxidized by $^*Ir^{III}$ to afford radical cation **IN0** and an Ir^{II} species in small amounts. Thus the newly obtained Ir^{II} intermediate (−0.69 V vs SCE in MeCN[15]) might be oxidized by PhtSCF$_3$ (−0.80 V vs SCE in MeCN[50]) to generate the initial Ir^{III} complex, bis(trifluoromethyl)disulfide, and phthalimide anion. Finally, proton transfer between phthalimide anion and **IN0** took place, leading to the formation of PhtH and the reactive amidyl radical **IN1**. Notably, the redox potential measurements of photocatalyst **A**, **8b**, and PhtSCF$_3$ were performed in MeCN whereas the three-component reaction did not occur in MeCN (Scheme 2h); hence, the solvent effect of PhCF$_3$ might also have a positive influence on the reaction.

For reactions conducted in the presence of $NBu_4OP(O)(OBu)_2$, instead of undergoing the endergonic electron transfer with the amide substrate, the photo-excited Ir^{III} intermediate (as an oxidant; $^*Ir^{III}/Ir^{II}$ = +1.68 V vs SCE in MeCN[15]) might have preferred to activate the amide substrate via PCET, cooperating with $(BuO)_2PO_2^-$ (as a base; pK_a = 13 in MeCN[15]) to furnish the reactive amidyl radical **IN1**, an Ir^{II} intermediate, and $(BuO)_2PO_2H$ (Figure 4b).[15] Subsequently, the Ir^{II} intermediate (−0.69 V vs SCE in MeCN[15]) might have been oxidized by PhtSCF$_3$ (−0.80 V vs SCE in MeCN[50]) to generate the initial Ir^{III} complex **A**, phthalimide anion, and bis(trifluoromethyl) disulfide. Finally, proton transfer between phthalimide anion and $(BuO)_2PO_2H$ could occur, leading to the formation of PhtH and the regeneration of $(BuO)_2PO_2^-$.

To further understand the radical cascade cyclization of amidyl radical **IN1**,[45] we performed DFT (UB3LYP)

DOI: 10.31635/ccschem.019.20190018
CCS Chem. **2019**, *1*, 352–364

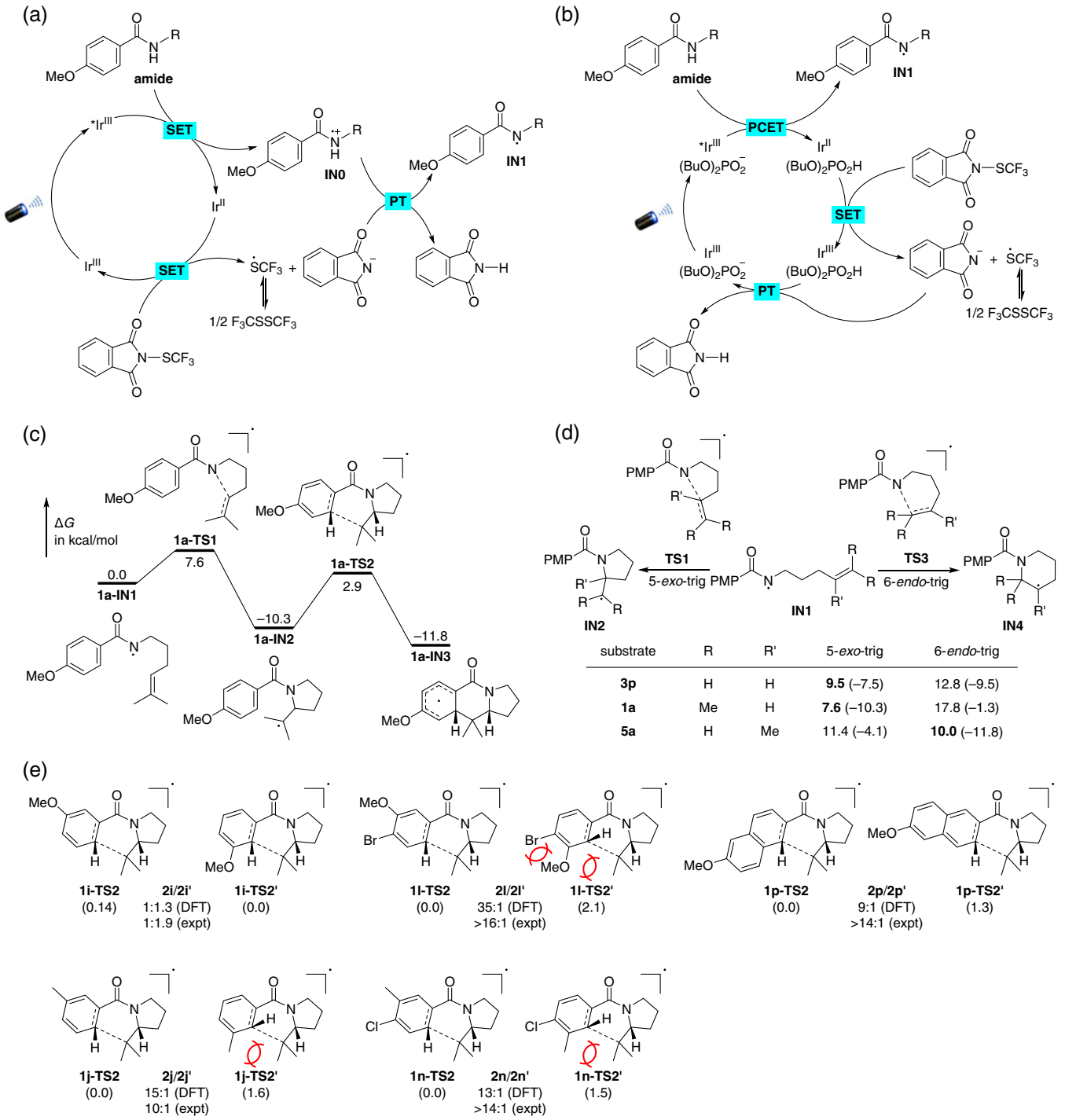

Figure 4 | *Proposed mechanism. (a) Possible reaction pathway for amidyl radical generation in the absence of $NBu_4OP(O)(OBu)_2$. (b) Possible reaction pathway for amidyl radical generation in the presence of $NBu_4OP(O)(OBu)_2$. (c) Gibbs energy profile for the radical cascade cyclization. (d) Regioselectivity of amidyl radical cyclization. Gibbs energies of activation are reported in kcal/mol. Gibbs energy changes are given in parentheses and reported in kcal/mol. (e) Regioselectivity of the intramolecular radical addition to aromatic rings. Relative Gibbs energies are given in parentheses and reported in kcal/mol. Computed at the UB3LYP/6-31+G(d,p) level. PT, proton transfer.*

calculations (Figure 4c). For substrate **1a**, amidyl radical **1a-IN1** underwent a fast exergonic 5-*exo*-trig cyclization (the Gibbs energy of activation for this step is 7.6 kcal/mol), generating tertiary carbon radical **1a-IN2**. Following this step, a subsequent intramolecular radical addition occurred to form dearomatized intermediate **1a-IN3** (the Gibbs energy of activation for this step is 13.2 kcal/mol), which finally underwent an oxidative aromatization

DOI: 10.31635/ccschem.019.20190018
CCS Chem. **2019**, *1*, 352–364

process or a hydrogen atom transfer with **1a-IN1** to furnish the tricyclic product **2a**.[45]

Accordingly, we investigated the regioselectivity of the amidyl radical cyclization (Figure 4d).[54-56] For substrates **3p** (R = R′ = H) and **1a** (R = Me, R′ = H), DFT calculations indicated that the 5-*exo*-trig cyclization was favored kinetically over the competing 6-*endo*-trig cyclization by 3.3 and 10.2 kcal/mol, respectively. In contrast, for substrate **5a** (R = H, R′ = Me), the 6-*endo*-trig cyclization was favored over the 5-*exo*-trig one by 1.4 kcal/mol. These computational results were in good agreement with our experimental observations (Figure 3). We reasoned that the reversal of regioselectivity of **5a** is due to the fact that the 6-*endo*-trig cyclization generated a stable tertiary radical, whereas the 5-*exo*-trig cyclization formed an unstable primary radical.

For substrates in Figure 3a,b, after the 5-*exo*-trig cyclization, the intramolecular radical addition to the aromatic ring was favored over the intermolecular trifluoromethylthiolation, possibly due to entropic reasons. In contrast, for substrates in Figure 3c, after the 6-*endo*-trig cyclization, the radical center of **IN4** was far away from the aromatic ring and could not undergo the intramolecular dearomatization, to generate an unstable twisted amide intermediate. Instead, **IN4** might undergo a similar reaction pathway as proposed by Glorius group to form the C–S bond and to complete the catalytic cycle.[51,52] As a result, only the trifluoromethylthiolated product **6** was observed experimentally.

Finally, the regioselectivity of intramolecular radical addition to the aromatic rings was also investigated (Figure 4e). For 3-methoxy substrate **1i**, the radical addition on the *ortho* position of the methoxy group is slightly favored over the *para* position by 0.14 kcal/mol, which is in accordance with the poor regioselectivity observed in the reaction of **1i**. In contrast, the reaction of 4-bromo-3-methoxy substrate **1l** was predicted to have a much better regiocontrol. We reasoned that in transition state **1i-TS2′** the methoxy group might have rotated to avoid the steric repulsion with the methyl substituents of the tertiary alkyl radical; however, an additional steric repulsion between the methoxy group and the bromo substituent in transition state **1l-TS2′** existed, resulting in the different regioselectivities observed in the reaction of substrates **1i** and **1l**. For 3-methyl substrate **1j**, the predicted ratio of **2j** to **2j′** was 15:1, which was close to the experimentally observed value (10:1). We reasoned that the steric repulsion between the methyl group on the aromatic ring and one methyl substituent of the tertiary alkyl radical disfavored the addition on the *ortho* position. An additional chloro substitution on the aromatic ring did not affect the regioselectivity significantly (the predicted ratios of **2j**/**2j′** and **2n**/**2n′** were 15:1 and 13:1, respectively), which was in agreement with the experimental results (Figure 3a). For naphthoyl substrate **1p**, the predicted ratio of α- to β-addition was 9:1, also consistent with the experiments (>14:1). These computational results demonstrated that both steric and electronic effects contributed to the regioselectivity of the aromatic radical addition step.

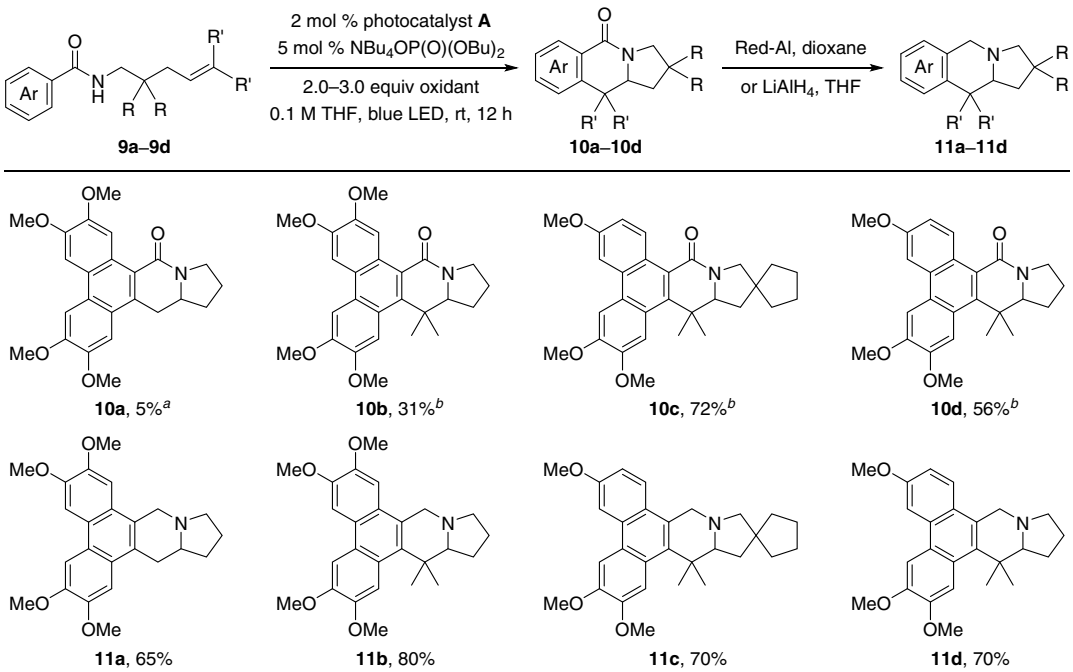

Figure 5 | *Synthesis of tylophorine and its analogues. Isolated yields. [a]Dilauroyl peroxide as the oxidant. [b]N-fluorobenzenesulfonimide as the oxidant.*

DOI: 10.31635/ccschem.019.20190018
CCS Chem. **2019**, *1*, 352–364

Synthetic Applications

Although phenanthroindolizidine alkaloids (e.g., tylophorine) have demonstrated diverse biological activities, their side effects on the central nervous system (CNS), poor solubility, and low metabolic stability have limited their applications severely.[57,58] A common strategy for improving the drug-like properties of natural products of clinical interest is to introduce a *gem*-dimethyl group.[59] However, due to limited synthetic methods, there was no accessible route for the *gem*-dimethyl analogues of tylophorine. With the newly developed photoredox-catalyzed aminoarylation in hand, we sought to apply it into the synthesis of tylophorine and its *gem*-dimethyl analogues. To our delight, as shown in Figure 5, our method could be implemented into a facile synthesis of **10a** albeit in only 5% yield and it was converted readily into natural product tylophorine (**11a**) after reduction. Remarkably, this strategy also provided a concise synthetic route for the *gem*-dimethyl analogues of tylophorine (**11b**–**11d**).

Encouragingly, our method has provided a promising strategy for improving the drug-like properties of this type of alkaloids. As shown in Table 2a, while the solubility of tylophorine was lower than 1 mM in dimethyl sulfoxide (DMSO), we found that the corresponding value of **11b** was higher than 30 mM, and what is more, those of **11c** and **11d** were more than 500 mM. The measured aqueous solubility of **11d** in phosphate-buffered saline (>200 μg/mL) was much better than that of tylophorine (<10 μg/mL), which might further lower its tendency to cross the blood–brain barrier, thereby, minimizing the CNS side effects. In another aspect, tylophorine easily decomposed in organic solvents (Supporting Information Figure S11).[44] In contrast, according to ^{1}H NMR analysis, our *gem*-dimethyl analogue **11c** showed no detectable degradation after at least 1 week, demonstrating that the installation of a bulky *gem*-dimethyl group led to a significant increase in its stability (Table 2b).

Table 2 | *Solubility and Stability Tests*

(a)

Compound	Solubility in DMSO (mM)	Aqueous Solubility[a] (μg/mL)
Tylophorine	<1	<10[b]
11b	>30	
11c	>500	
11d	>500	>200

(b)

Compound	Time	Stability
Tylophorine	1 day	Some degradation
	1 week	Serious degradation
11c	1 week	No degradation

[a]Aqueous solubility was tested in phosphate buffered saline (pH = 7.2–7.4).
[b]Tested solubility data were in agreement with literature reported value.[44]

Experimental Methods

General Procedure for Photoredox-Catalyzed Alkene Aminoarylation

An oven-dried 2 mL screw-capped vial was equipped with a magnetic stirring bar, and then benzamide (0.1–0.2 mmol), $PhtSCF_3$ (1.5–2.5 equiv), tetrabutylammonium dibutyl phosphate (5 mol %), $[Ir(dF(CF_3)ppy)_2(dCF_3bpy)]PF_6$ (2 mol %), and dry $PhCF_3$ (0.1 M) were added. The resulting mixture was degassed using three freeze–pump–thaw cycles and finally backfilled with argon. After that, the reaction mixture was allowed to stir at room temperature for 12–40 h under irradiation from a 10 W blue light-emitting diode, equipped with a cooling fan to allow even temperature distribution. Following filtration of the mixture, the filtrate was concentrated and purified by column chromatography, using petroleum ether (PE) and ethyl acetate (EA) (PE:EA = 2:1–1:1) as the solvent system, on 200–300 mesh silica gel to afford the desired product.

Computational Methods

All DFT calculations were performed with Gaussian 09.[60] Pruned integration grids with 99 radial shells and 590 angular points per shell were used. Geometry optimizations of the stationary points were carried out at the UB3LYP/6-31+G(d,p) level without any constrains.[61–63] Unscaled harmonic frequency calculations were performed at the same level to validate each structure as either a minimum or a transition state, and to evaluate its zero-point energy and thermal corrections at 298 K. Quasiharmonic corrections were applied during the entropy calculations by setting all positive frequencies that are less than 100 cm^{-1} to 100 cm^{-1}.[64,65] All indicated energy differences were based on Gibbs energies in the gas phase, with the standard temperature of 298 K, and the hypothetical pressure state of 1 atm.

Conclusions

Our present study reports novel approaches for photoredox-catalyzed aminoarylation and thioamination of unactivated alkenes with *N*-alkyl benzamides. These new methodologies provide facile and concise synthetic routes to access synthetically challenging quaternary carbon-centered benzoindolizidinones and functionalized piperidines. The selective generation of five- and six-membered N-heterocycles could be finely tuned by the substitution pattern of the substrates. DFT

DOI: 10.31635/ccschem.019.20190018
CCS Chem. **2019**, *1*, 352–364

calculations were performed to understand the reaction mechanism and to rationalize the regioselectivities. Moreover, the newly developed catalytic aminoarylation presents a convenient synthetic advancement for tylophorine and its *gem*-dimethyl analogues. The exploitation of the bulky *gem*-dimethyl group achieved favorable drug-like properties, such as substantial improvement of solubility and stability.

Supporting Information

Supporting Information is available, which includes additional experimental procedures, characterization data, copies of NMR spectra, and computational data.

Conflicts of Interest

The authors declare no competing financial interests.

Funding Information

This study was funded by the National "973" grant from the Ministry of Science and Technology (grant no. 2011CB965300), National Natural Science Foundation of China (grant nos. 21232001 and 21302106), National Science and Technology Major Project (grant no. 2018ZX09711001), and Tsinghua University Initiative Scientific Research Program.

Acknowledgments

We are grateful to Prof. Zongxiu Nie for his assistance with high-resolution mass spectrometry experiments. We thank Prof. Qingmin Wang and Prof. Sidney M. Hecht for their helpful discussions.

References

1. Huryn, D. M.; Wipf, P. Natural Product Chemistry and Anticancer Drug Discovery. In *Cancer Drug Design and Discovery*, 2nd ed.; Neidle, S., Ed.; Academic Press: New York, **2014**; Part II, Chapter 3; pp 91–120.
2. Vitaku, E.; Smith, D. T.; Njardarson, J. T. Analysis of the Structural Diversity, Substitution Patterns, and Frequency of Nitrogen Heterocycles among U.S. FDA Approved Pharmaceuticals. *J. Med. Chem.* **2014**, *57*, 10257–10274.
3. Vo, C.-V. T.; Bode, J. W. Synthesis of Saturated N-Heterocycles. *J. Org. Chem.* **2014**, *79*, 2809–2815.
4. Chen, J.-R.; Hu, X.-Q.; Lu, L.-Q.; Xiao, W.-J. Exploration of Visible-Light Photocatalysis in Heterocycle Synthesis and Functionalization: Reaction Design and Beyond. *Acc. Chem. Res.* **2016**, *49*, 1911–1923.
5. Zard, S. Z. Recent Progress in the Generation and Use of Nitrogen-Centred Radicals. *Chem. Soc. Rev.* **2008**, *37*, 1603–1618.
6. Chen, J.-R.; Hu, X.-Q.; Lu, L.-Q.; Xiao, W.-J. Visible Light Photoredox-Controlled Reactions of N-Radicals and Radical Ions. *Chem. Soc. Rev.* **2016**, *45*, 2044–2056.
7. Jiang, H.; Studer, A. Chemistry with N-Centered Radicals Generated by Single-Electron Transfer-Oxidation Using Photoredox Catalysis. *CCS Chem.* **2019**, *1*, 38–49.
8. Hu, X.-Q.; Qi, X.; Chen, J.-R.; Zhao, Q.-Q.; Wei, Q.; Lan, Y.; Xiao, W.-J. Catalytic N-Radical Cascade Reaction of Hydrazones by Oxidative Deprotonation Electron Transfer and TEMPO Mediation. *Nat. Commun.* **2016**, *7*, 11188.
9. Jiang, H.; Studer, A. Iminyl-Radicals by Oxidation of α-Imino-oxy Acids: Photoredox-Neutral Alkene Carboimination for the Synthesis of Pyrrolines. *Angew. Chem. Int. Ed.* **2017**, *56*, 12273–12276.
10. Davies, J.; Sheikh, N. S.; Leonori, D. Photoredox Imino Functionalizations of Olefins. *Angew. Chem. Int. Ed.* **2017**, *56*, 13361–13365.
11. Wang, X.; Xia, D.; Qin, W.; Zhou, R.; Zhou, X.; Zhou, Q.; Liu, W.; Dai, X.; Wang, H.; Wang, S.; Tan, L.; Zhang, D.; Song, H.; Liu, X.-Y.; Qin, Y. A Radical Cascade Enabling Collective Syntheses of Natural Products. *Chem* **2017**, *2*, 803–816.
12. Wang, Y.; Hu, X.; Morales-Rivera, C. A.; Li, G.-X.; Huang, X.; He, G.; Liu, P.; Chen, G. Epimerization of Tertiary Carbon Centers via Reversible Radical Cleavage of Unactivated C(sp^3)–H Bonds. *J. Am. Chem. Soc.* **2018**, *140*, 9678–9684.
13. Choi, G. J.; Knowles, R. R. Catalytic Alkene Carboaminations Enabled by Oxidative Proton-Coupled Electron Transfer. *J. Am. Chem. Soc.* **2015**, *137*, 9226–9229.
14. Miller, D. C.; Choi, G. J.; Orbe, H. S.; Knowles, R. R. Catalytic Olefin Hydroamidation Enabled by Proton-Coupled Electron Transfer. *J. Am. Chem. Soc.* **2015**, *137*, 13492–13495.
15. Choi, G. J.; Zhu, Q.; Miller, D. C.; Gu, C. J.; Knowles, R. R. Catalytic Alkylation of Remote C–H Bonds Enabled by Proton-Coupled Electron Transfer. *Nature* **2016**, *539*, 268–271.
16. Chu, J. C. K.; Rovis, T. Amide-Directed Photoredox-Catalysed C–C Bond Formation at Unactivated sp^3 C–H Bonds. *Nature* **2016**, *539*, 272–275.
17. Chen, D.-F.; Chu, J. C. K.; Rovis, T. Directed γ-C(sp^3)–H Alkylation of Carboxylic Acid Derivatives through Visible Light Photoredox Catalysis. *J. Am. Chem. Soc.* **2017**, *139*, 14897–14900.
18. Zhu, Q.; Graff, D. E.; Knowles, R. R. Intermolecular Anti-Markovnikov Hydroamination of Unactivated Alkenes with Sulfonamides Enabled by Proton-Coupled Electron Transfer. *J. Am. Chem. Soc.* **2018**, *140*, 741–747.
19. Davies, J.; Svejstrup, T. D.; Reina, D. F.; Sheikh, N. S.; Leonori, D. Visible-Light-Mediated Synthesis of Amidyl Radicals: Transition-Metal-Free Hydroamination and N-Arylation Reactions. *J. Am. Chem. Soc.* **2016**, *138*, 8092–8095.
20. Wu, K.; Wang, L.; Colón-Rodríguez, S.; Flechsig, G.-U.; Wang, T. Amidyl Radical Directed Remote Allylation of Unactivated sp^3 C–H Bonds via Organic Photoredox Catalysis. *Angew. Chem. Int. Ed.* **2018**, *58*, 1774–1778.
21. Xia, Y.; Wang, L.; Studer, A. Site-Selective Remote Radical C–H Functionalization of Unactivated C–H Bonds in

Amides Using Sulfone Reagents. *Angew. Chem. Int. Ed.* **2018**, *57*, 12940–12944.
22. Chen, Q.; Shen, M.; Tang, Y.; Li, C. Cyclization or Hydrogen Migration: Theoretical Study and Experimental Evidence on the Reactivities of Unsaturated Amidyl Radicals. *Org. Lett.* **2005**, *7*, 1625–1627.
23. Hu, T.; Shen, M.; Chen, Q.; Li, C. Pushing Radical Cyclization from Regioselective to Regiospecific: Cyclization of Amidyl Radicals Controlled by Vinylic Halogen Substitution. *Org. Lett.* **2006**, *8*, 2647–2650.
24. Zhuang, S.; Liu, K.; Li, C. Stereoselective 6-Exo Cyclization of Amidyl Radicals. An Experimental and Theoretical Study. *J. Org. Chem.* **2011**, *76*, 8100–8106.
25. Li, Z.; Song, L.; Li, C. Silver-Catalyzed Radical Aminofluorination of Unactivated Alkenes in Aqueous Media. *J. Am. Chem. Soc.* **2013**, *135*, 4640–4643.
26. Xu, H.-C.; Moeller, K. D. Intramolecular Anodic Olefin Coupling Reactions: The Use of a Nitrogen Trapping Group. *J. Am. Chem. Soc.* **2008**, *130*, 13542–13543.
27. Zhu, L.; Xiong, P.; Mao, Z.-Y.; Wang, Y.-H.; Yan, X.; Lu, X.; Xu, H.-C. Electrocatalytic Generation of Amidyl Radicals for Olefin Hydroamidation: Use of Solvent Effects to Enable Anilide Oxidation. *Angew. Chem. Int. Ed.* **2016**, *55*, 2226–2229.
28. Hou, Z.-W.; Mao, Z.-Y.; Zhao, H.-B.; Melcamu, Y. Y.; Lu, X.; Song, J.; Xu, H.-C. Electrochemical C–H/N–H Functionalization for the Synthesis of Highly Functionalized (Aza)indoles. *Angew. Chem. Int. Ed.* **2016**, *55*, 9168–9172.
29. Xiong, P.; Xu, H.-H.; Xu, H.-C. Metal- and Reagent-Free Intramolecular Oxidative Amination of Tri- and Tetrasubstituted Alkenes. *J. Am. Chem. Soc.* **2017**, *139*, 2956–2959.
30. Hou, Z.-W.; Mao, Z.-Y.; Melcamu, Y. Y.; Lu, X.; Xu, H.-C. Electrochemical Synthesis of Imidazo-Fused N-Heteroaromatic Compounds through a C–N Bond-Forming Radical Cascade. *Angew. Chem. Int. Ed.* **2018**, *57*, 1636–1639.
31. Hou, Z.-W.; Yan, H.; Song, J.-S.; Xu, H.-C. Electrochemical Synthesis of (Aza)indolines via Dehydrogenative [3+2] Annulation: Application to Total Synthesis of (±)-Hinckdentine A. *Chin. J. Chem.* **2018**, *36*, 909–915.
32. Xu, F.; Long, H.; Song, J.; Xu, H.-C. De Novo Synthesis of Highly Functionalized Benzimidazolones and Benzoxazolones through an Electrochemical Dehydrogenative Cyclization Cascade. *Angew. Chem. Int. Ed.* **2019**, *58*, 9017–9021.
33. Tucker, J. W.; Stephenson, C. R. J. Shining Light on Photoredox Catalysis: Theory and Synthetic Applications. *J. Org. Chem.* **2012**, *77*, 1617–1622.
34. Prier, C. K.; Rankic, D. A.; MacMillan, D. W. C. Visible Light Photoredox Catalysis with Transition Metal Complexes: Applications in Organic Synthesis. *Chem. Rev.* **2013**, *113*, 5322–5363.
35. Tellis, J. C.; Kelly, C. B.; Primer, D. N.; Jouffroy, M.; Patel, N. R.; Molander, G. A. Single-Electron Transmetalation via Photoredox/Nickel Dual Catalysis: Unlocking a New Paradigm for sp^3–sp^2 Cross-Coupling. *Acc. Chem. Res.* **2016**, *49*, 1429–1439.
36. Romero, N. A.; Nicewicz, D. A. Organic Photoredox Catalysis. *Chem. Rev.* **2016**, *116*, 10075–10166.
37. Kärkäs, M. D. Photochemical Generation of Nitrogen-Centered Amidyl, Hydrazonyl, and Imidyl Radicals: Methodology Developments and Catalytic Applications. *ACS Catal.* **2017**, *7*, 4999–5022.
38. Strieth-Kalthoff, F.; James, M. J.; Teders, M.; Pitzer, L.; Glorius, F. Energy Transfer Catalysis Mediated by Visible Light: Principles, Applications, Directions. *Chem. Soc. Rev.* **2018**, *47*, 7190–7202.
39. Weinberg, D. R.; Gagliardi, C. J.; Hull, J. F.; Murphy, C. F.; Kent, C. A.; Westlake, B. C.; Paul, A.; Ess, D. H.; McCafferty, D. G.; Meyer, T. J. Proton-Coupled Electron Transfer. *Chem. Rev.* **2012**, *112*, 4016–4093.
40. Gentry, E. C.; Knowles, R. R. Synthetic Applications of Proton-Coupled Electron Transfer. *Acc. Chem. Res.* **2016**, *49*, 1546–1556.
41. Gellert, E. The Indolizidine Alkaloids. *J. Nat. Prod.* **1982**, *45*, 50–73.
42. Gao, W.; Lam, W.; Zhong, S.; Kaczmarek, C.; Baker, D. C.; Cheng, Y.-C. Novel Mode of Action of Tylophorine Analogs as Antitumor Compounds. *Cancer Res.* **2004**, *64*, 678–688.
43. Wen, T.; Wang, Z.; Meng, X.; Wu, M.; Li, Y.; Wu, X.; Zhao, L.; Wang, P.; Yin, Z.; Li-Ling, J.; Wang, Q. Synthesis of Novel Tylophorine Derivatives and Evaluation of Their Anti-Inflammatory Activity. *ACS Med. Chem. Lett.* **2014**, *5*, 1027–1031.
44. Han, G.; Chen, L.; Wang, Q.; Wu, M.; Liu, Y.; Wang, Q. Design, Synthesis, and Antitobacco Mosaic Virus Activity of Water-Soluble Chiral Quaternary Ammonium Salts of Phenanthroindolizidines Alkaloids. *J. Agric. Food Chem.* **2018**, *66*, 780–788.
45. Newcomb, M.; Esker, J. L. Facile Production and Cyclizations of Amidyl Radicals. *Tetrahedron Lett.* **1991**, *32*, 1035–1038.
46. Orito, K.; Miyazawa, M.; Nakamura, T.; Horibata, A.; Ushito, H.; Nagasaki, H.; Yuguchi, M.; Yamashita, S.; Yamazaki, T.; Tokuda, M. $Pd(OAc)_2$-Catalyzed Carbonylation of Amines. *J. Org. Chem.* **2006**, *71*, 5951–5958.
47. Bertrand, M. B.; Leathen, M. L.; Wolfe, J. P. Mild Conditions for the Synthesis of Functionalized Pyrrolidines via Pd-Catalyzed Carboamination Reactions. *Org. Lett.* **2007**, *9*, 457–460.
48. Müller, T. E.; Beller, M. Metal-Initiated Amination of Alkenes and Alkynes. *Chem. Rev.* **1998**, *98*, 675–704.
49. Ruccolo, S.; Qin, Y.; Schnedermann, C.; Nocera, D. G. General Strategy for Improving the Quantum Efficiency of Photoredox Hydroamidation Catalysis. *J. Am. Chem. Soc.* **2018**, *140*, 14926–14937.
50. Xu, W.; Ma, J.; Yuan, X.-A.; Dai, J.; Xie, J.; Zhu, C. Synergistic Catalysis for the Umpolung Trifluoromethylthiolation of Tertiary Ethers. *Angew. Chem. Int. Ed.* **2018**, *57*, 10357–10361.
51. Mukherjee, S.; Maji, B.; Tlahuext-Aca, A.; Glorius, F. Visible-Light-Promoted Activation of Unactivated $C(sp^3)$–H Bonds and their Selective Trifluoromethylthiolation. *J. Am. Chem. Soc.* **2016**, *138*, 16200–16203.
52. Mukherjee, S.; Patra, T.; Glorius, F. Cooperative Catalysis: A Strategy to Synthesize Trifluoromethylthioesters from Aldehydes. *ACS Catal.* **2018**, *8*, 5842–5846.

53. Roth, H. G.; Romero, N. A.; Nicewicz, D. A. Experimental and Calculated Electrochemical Potentials of Common Organic Molecules for Applications to Single-Electron Redox Chemistry. *Synlett* **2016**, *27*, 714–723.
54. Lu, H.; Chen, Q.; Li, C. Control of the Regioselectivity of Sulfonamidyl Radical Cyclization by Vinylic Halogen Substitution. *J. Org. Chem.* **2007**, *72*, 2564–2569.
55. Yu, Y.-Y.; Fu, Y.; Xie, M.; Liu, L.; Guo, Q.-X. Controlling Regioselectivity in Cyclization of Unsaturated Amidyl Radicals: 5-Exo Versus 6-Endo. *J. Org. Chem.* **2007**, *72*, 8025–8032.
56. Yuan, X.; Liu, K.; Li, C. Development of Highly Regioselective Amidyl Radical Cyclization Based on Lone Pair–Lone Pair Repulsion. *J. Org. Chem.* **2008**, *73*, 6166–6171.
57. Wei, L.; Shi, Q.; Bastow, K. F.; Brossi, A.; Morris-Natschke, S. L.; Nakagawa-Goto, K.; Wu, T.-S.; Pan, S.-L.; Teng, C.-M.; Lee, K.-H. Antitumor Agents 253. Design, Synthesis, and Antitumor Evaluation of Novel 9-Substituted Phenanthrene-Based Tylophorine Derivatives as Potential Anticancer Agents. *J. Med. Chem.* **2007**, *50*, 3674–3680.
58. Lee, Y.-Z.; Yang, C.-W.; Hsu, H.-Y.; Qiu, Y.-Q.; Yeh, T.-K.; Chang, H.-Y.; Chao, Y.-S.; Lee, S.-J. Synthesis and Biological Evaluation of Tylophorine-Derived Dibenzoquinolines as Orally Active Agents: Exploration of the Role of Tylophorine E Ring on Biological Activity. *J. Med. Chem.* **2012**, *55*, 10363–10377.
59. Talele, T. T. Natural-Products-Inspired Use of the gem-Dimethyl Group in Medicinal Chemistry. *J. Med. Chem.* **2018**, *61*, 2166–2210.
60. Frisch, M. J.; Trucks, G. W.; Schlegel, H. B.; Scuseria, G. E.; Robb, M. A.; Cheeseman, J. R.; Scalmani, G.; Barone, V.; Mennucci, B.; Petersson, G. A.; Nakatsuji, H.; Caricato, M.; Li, X.; Hratchian, H. P.; Izmaylov, A. F.; Bloino, J.; Zheng, G.; Sonnenberg, J. L.; Hada, M.; Ehara, M.; Toyota, K.; Fukuda, R.; Hasegawa, J.; Ishida, M.; Nakajima, T.; Honda, Y.; Kitao, O.; Nakai, H.; Vreven, T.; Montgomery, J. A., Jr.; Peralta, J. E.; Ogliaro, F.; Bearpark, M.; Heyd, J. J.; Brothers, E.; Kudin, K. N.; Staroverov, V. N.; Keith, T.; Kobayashi, R.; Normand, J.; Raghavachari, K.; Rendell, A.; Burant, J. C.; Iyengar, S. S.; Tomasi, J.; Cossi, M.; Rega, N.; Millam, J. M.; Klene, M.; Knox, J. E.; Cross, J. B.; Bakken, V.; Adamo, C.; Jaramillo, J.; Gomperts, R.; Stratmann, R. E.; Yazyev, O.; Austin, A. J.; Cammi, R.; Pomelli, C.; Ochterski, J. W.; Martin, R. L.; Morokuma, K.; Zakrzewski, V. G.; Voth, G. A.; Salvador, P.; Dannenberg, J. J.; Dapprich, S.; Daniels, A. D.; Farkas, Ö.; Foresman, J. B.; Ortiz, J. V.; Cioslowski, J.; Fox, D. J. *Gaussian 09, Revision E.01,* Gaussian, Inc.: Wallingford, CT, **2013**.
61. Lee, C.; Yang, W.; Parr, R. G. Development of the Colle-Salvetti Correlation-Energy Formula into a Functional of the Electron Density. *Phys. Rev. B* **1988**, *37*, 785–789.
62. Becke, A. D. Density-Functional Thermochemistry. III. The Role of Exact Exchange. *J. Chem. Phys.* **1993**, *98*, 5648–5652.
63. Hehre, W. J.; Radom, L.; Schleyer, P. V. R.; Pople, J. A. *Ab Initio Molecular Orbital Theory,* Wiley: New York, **1986**.
64. Zhao, Y.; Truhlar, D. G. Computational Characterization and Modeling of Buckyball Tweezers: Density Functional Study of Concave-Convex $\pi\cdots\pi$ Interactions. *Phys. Chem. Chem. Phys.* **2008**, *10*, 2813–2818.
65. Ribeiro, R. F.; Marenich, A. V.; Cramer, C. J.; Truhlar, D. G. Use of Solution-Phase Vibrational Frequencies in Continuum Models for the Free Energy of Solvation. *J. Phys. Chem. B* **2011**, *115*, 14556–14562.

DOI: 10.31635/ccschem.019.20190018
CCS Chem. **2019**, *1*, 352–364